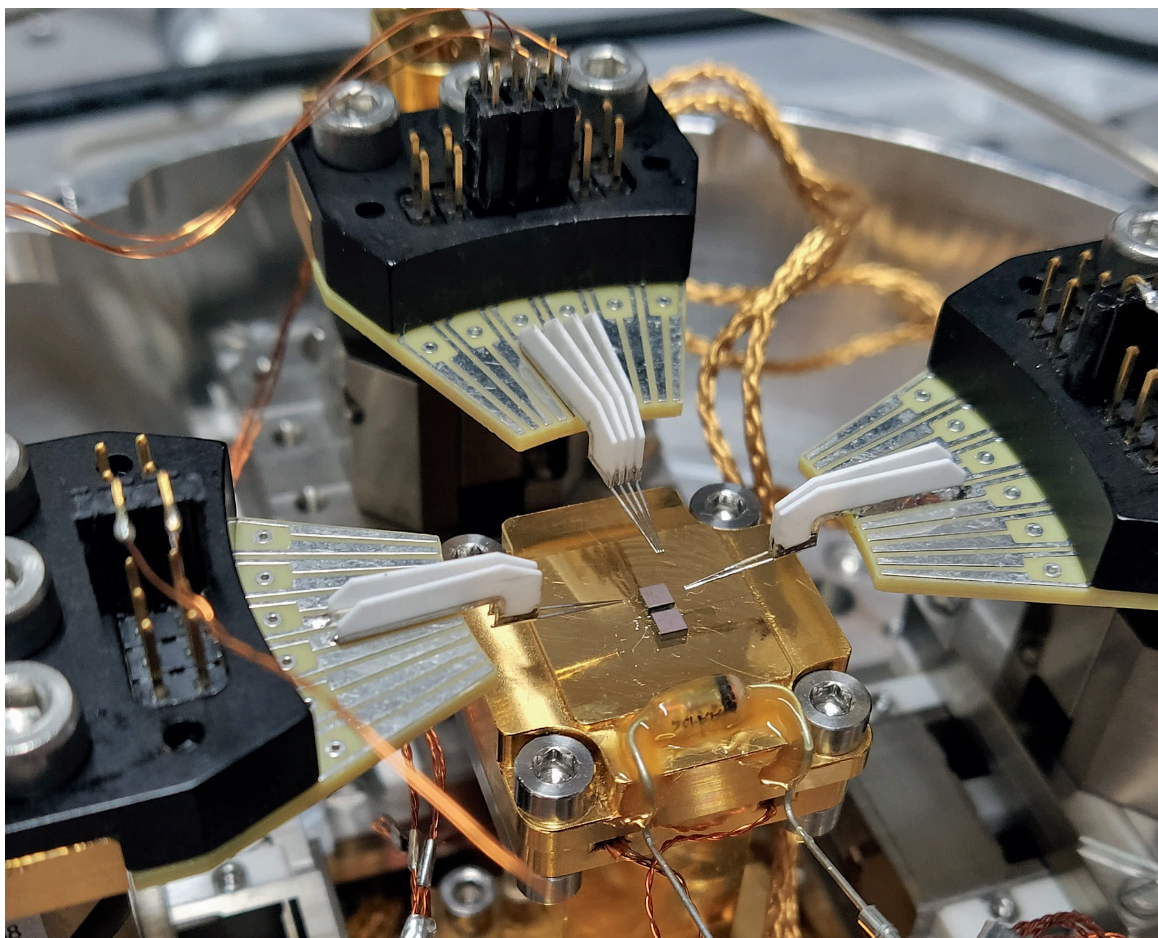

DC and RF characterization of bulk CMOS and FD-SOI devices at cryogenic temperatures with respect to quantum computing applications

Anton Artanov

Information
Band / Volume 93
ISBN 978-3-95806-687-8

Mitglied der Helmholtz-Gemeinschaft

JÜLICH
Forschungszentrum

Forschungszentrum Jülich GmbH
Zentralinstitut für Engineering, Elektronik und Analytik (ZEA)
Systeme der Elektronik (ZEA-2)

DC and RF characterization of bulk CMOS and FD-SOI devices at cryogenic temperatures with respect to quantum computing applications

Anton Artanov

Schriften des Forschungszentrums Jülich
Reihe Information / Information Band / Volume 93

ISSN 1866-1777 ISBN 978-3-95806-687-8

Contents

Acknowledgement **i**

Abstract **iii**

Zusammenfassung **v**

List of Figures **ix**

List of Tables **xiii**

Acronyms **xv**

1 Introduction **1**
- 1.1 Motivation 1
- 1.2 Structure of this work 2

2 Fundamentals **3**
- 2.1 Quantum computing 3
  - 2.1.1 Dirac notation 3
  - 2.1.2 Quantum bits 4
  - 2.1.3 Bloch sphere 4
  - 2.1.4 Quantum computer requirements 5
- 2.2 Cryogenic CMOS 6

3 Cryogenic measurement setup **9**
- 3.1 Cooling methods 9
  - 3.1.1 Immersion into a cryogen 9
  - 3.1.2 Bath cryostat 11
  - 3.1.3 Closed-cycle cryostat 12
- 3.2 Requirements 13
- 3.3 Setup description 14
- 3.4 Setup characterization 16
  - 3.4.1 Thermal properties 16
  - 3.4.2 DC properties 19
  - 3.4.3 RF properties 19
  - 3.4.4 Conclusions 21

4 Test devices design **23**
- 4.1 Fabrication technology choice 23
- 4.2 SQuBiC2 – 65 nm bulk CMOS 24
- 4.3 SQuBiC5 – 22 nm FD-SOI 26
- 4.4 Conclusions 27

6.4 Comparison of the simulated (dashed lines) and measured (solid lines) scattering parameters data of the transistor array [81]. 42
6.5 Small-signal equivalent circuit of a de-embedded single FDSOI MOSFET device (adopted from [88]). 44
6.6 Small-signal equivalent circuits in quasi-static operation (adopted from [88]). 45
6.7 Gate-source capacitance extraction: blue - W = 2.4 μm, red - W = 4.8 μm, yellow - W = 9.6 μm. 48
6.8 Gate-drain capacitance extraction: blue - W = 2.4 μm, red - W = 4.8 μm, yellow - W = 9.6 μm. 49
6.9 Drain-source capacitance extraction: blue - W = 2.4 μm, red - W = 4.8 μm, yellow - W = 9.6 μm. 50
6.10 Transconductance g_m and drain-source conductance g_{ds} extraction: blue - W = 2.4 μm, red - W = 4.8 μm, yellow - W = 9.6 μm. 51
6.11 The comparison of the simulated with extracted SSEC (dashed lines) and measured (solid lines) scattering parameters data of the nMOS-FET array, W = 4.8 μm. 52
6.12 The extrapolations of H_{21} and U for three nMOS devices at 300 K and 6 K [81]. 53
6.13 Schematic representation of the cryogenic noise measurement chain. 59
6.14 Schematic representation of the input chain with cryogenic attenuator. . . . 59
6.15 Minimum DUT input noise temperature required for the condition of DUT output power to be above the receiver noise level, for the nFET with W = 2.4 μm [81]. 60
6.16 Noise measurements of two transistor arrays at room temperature. [81]. . . 61
6.17 Noise measurement at different temperatures for W = 9.6 μm transistor array [81]. 61

7.1 The principle schemes, showing four thermal paths of the n-type transistor, fabricated in 65 nm bulk CMOS (left) and 22 nm FD-SOI (right) technologies. 64
7.2 Layout scheme of the measured samples. 64
7.3 Photo of the working area of the setup. 64
7.4 Dependence of gate polysilicon resistance and temperature on voltage drop. 65
7.5 Dependence of gate polysilicon resistance and temperature measurement sensitivity on ambient temperature. 66
7.6 Measured $I_{ds} - V_{gs}$ characteristics and incremental temperature ΔT versus V_{gs} for samples in both fabrication technologies. 66
7.7 Measured incremental temperatures ΔT versus Joule power P at several ambient temperature values T_A for samples in both fabrication technologies. . . 67
7.8 Specific thermal resistance R^*_{th} versus temperature for different materials [113, 114, 115, 116, 117, 118]. 68
7.9 Extracted thermal resistance R_{th} seen from the gate as a function of the temperature T_M measured at the gate, 65 nm bulk CMOS [107]. 70
7.10 Calculated and measured channel temperature increase as a function of the dissipated power for several T_A, 65 nm bulk CMOS [107]. 70
7.11 Calculated and measured channel temperature increase as a function of the dissipated power at different bias conditions, 65 nm bulk CMOS [107]. 71
7.12 Dependency of the thermal resistance R_{th} (linear regime), seen from the gate side, on drain-source voltage V_{ds} for several ambient temperatures T_A [107]. . 71

7.13 Extracted thermal resistance R_{th} seen from the gate as a function of the temperature T_M measured at the gate, 22 nm FD-SOI. 72
7.14 Calculated and measured channel temperature increase as a function of the dissipated power for several T_A, 22 nm FD-SOI. 72
7.15 Simplified temperature distribution scheme. 74
7.16 Modeled dependence of temperature versus distance from the hotspot. . . . 75
7.17 Measured incremental temperatures ΔT of one structure versus Joule power P, produced by other structures on the chip. 76
7.18 Measured incremental temperatures ΔT versus Joule power P for the same 65 nm structure, mounted by two types of glue. 76

Information
Band / Volume 93
ISBN 978-3-95806-687-8

Mitglied der Helmholtz-Gemeinschaft